NASA TECHNICAL MEMORANDUM

NASA TM X-73402

NASA TM X-73402

LONGITUDINAL RESIDUAL STRESSES IN BORON FIBERS

by D. R. Behrendt
Lewis Research Center
Cleveland, Ohio 44135

TECHNICAL PAPER to be presented at
the Symposium on Composite Materials Testing and Design - Fourth Conference sponsored by the American Society for Testing and Materials
Valley Forge, Pennsylvania, May 3-4, 1976

1. Report No.	2. Government Accession No.	3. Recipient's Catalog No.
NASA TM X-73402		

4. Title and Subtitle	5. Report Date
LONGITUDINAL RESIDUAL STRESSES IN BORON FIBERS	6. Performing Organization Code
7. Author(s)	8. Performing Organization Report No.
D. R. Behrendt	E-8725
	10. Work Unit No.
9. Performing Organization Name and Address	
Lewis Research Center National Aeronautics and Space Administration Cleveland, Ohio 44135	11. Contract or Grant No.
	13. Type of Report and Period Covered
12. Sponsoring Agency Name and Address	Technical Memorandum
National Aeronautics and Space Administration Washington, D.C. 20546	14. Sponsoring Agency Code

15. Supplementary Notes

16. *Abstract*

A method of measuring the longitudinal residual stress distribution in boron fibers is presented. The residual stresses in commercial CVD boron on tungsten fibers of 102, 142, and 203 μm (4, 5.6, and 8 mil) diameters were determined. Results for the three sizes show a compressive stress at the surface [-800 to -1400 MN/m^2 (-120 to -200 ksi)], changing monotonically to a region of tensile stress within the boron. At ~25 percent of the original radius, the stress reaches a maximum tensile [600 to 1000 MN/m^2 (90 to 150 ksi)] and then decreases to compressive near the tungsten boride core. The core itself is under a compressive stress of ~-1300 MN/m^2 (-190 ksi). The effects of surface removal on core residual stress and core-initiated fracture are discussed.

17. Key Words (Suggested by Author(s))	18. Distribution Statement
Boron fibers; Residual stresses; Tungsten boride core; Fracture stress; Composites	Unclassified - unlimited

19. Security Classif. (of this report)	20. Security Classif. (of this page)	21. No. of Pages	22. Price*
Unclassified	Unclassified		

* For sale by the National Technical Information Service, Springfield, Virginia 22161

LONGITUDINAL RESIDUAL STRESSES IN BORON FIBERS

D. R. Behrendt

Modern boron fibers are produced by chemical vapor deposition (CVD) of boron from a BCl_3-H_2 gas mixture on a tungsten wire at high temperatures 1223 to 1573°K (1742 to 2372°F). At these temperatures, the boron diffuses into the tungsten, forming a core of several of the tungsten borides surrounded by a boron sheath. The tensile fracture strength of a brittle material such as the boron fiber depends on the size and distribution of flaws and on the residual stresses at these flaws. The high strength of boron fibers are due in part to the fact that the primary flaws are located at the surface and in the tungsten boride core, where residual stresses have been found to be compressive [1, 2, 3].

The residual stresses in Refs 1 and 3 were calculated from the radius of curvature of longitudinally split fibers by assuming a linear relation between stress and radius in the boron sheath. The compressive nature of the core stress was deduced from the decrease in the radius of curvature upon removal of the core by etching. In Ref 2, measurements of the change in length of a fiber upon etching of the surface along with the assumption that this change in length varied as the square of the radius were used to calculate the residual stresses. The purpose of the research reported here was to make continuous and more accurate determinations of the residual stress distributions in boron fibers with the goal of using the better understanding to show the way to produce stronger and more uniform fibers.

Experimental Test Apparatus

The experimental apparatus was designed so that continuous measurements could be made of the length changes of a boron fiber specimen as the surface of the fiber was removed by electropolishing. From these axial strains, the axial residual stress distribution could be calculated. As indicated in the schematic representation of the experimental apparatus (shown in Fig. 1),

the specimen is mounted between an inner and an outer quartz tube. The inner tube is free to slide within the outer tube in teflon bearings. The boron fiber to be tested is cemented with conducting epoxy between the bottom of the outer tube and a sleeve connected to the inner tube. The fiber test section is about 1 cm long. The center plate of a three-plate capacitor is attached to the top of the inner tube. The other two plates are insulated from each other and attached to the top of the outer tube. Thus, any changes in length of the specimen produced an equal change in the position of the center plate with respect to the outer plates. The relative position of the center plate is detected by applying a -100V peak-to-peak 3000 Hz voltage to the outer plates and feeding the resulting signal from the center plate into a high impedence (10 meg Ω) pre-amplifier and then to a lock-in amplifier. A strip chart recorder was connected to the output of the lock-in amplifier so that a continuous recording of length vs. time could be made.

The surface of the boron is removed by electropolishing at room temperature by placing the lower portion of the apparatus in a low conductivity solution made by dissolving 0.5 gm of NaOH in 30 cc of H_2O and adding this to 150 cc of glycerin. A current of 4 ma per centimeter of fiber length is maintained between the boron fiber and a concentric stainless steel cathode. By direct measurement of the fiber diameter at intervals during preliminary tests, it was established that the rate of mass removal from the fiber is constant for a given current and independent of fiber diameter. For a current of 4 ma/cm at $\sim$ 25 V, the mass removal rate was 6.3×10^{-8} gm/cm/sec. Using this information in an actual run, the fiber diameter for any time during the run could be calculated to an accuracy of 3% from a measurement of the final diameter and total time of electropolishing at constant current. This allowed the apparatus to be undisturbed during an actual run since physical

diameter measurements during the run were not necessary.

The advantages in using electropolishing instead of chemical etching are: (1) the electropolishing is done at room temperature whereas the chemical etching of boron usually requires temperatures near 373°K (212°F) to obtain sufficiently large etching rates, (2) the electropolishing method produces a more uniform removal of the surface. A scanning electron microscope was used to examine the surfaces of boron fibers in the as-received, lightly electropolished, and lightly etched [two parts nitric acid to one part water at 363°K (194°F)] conditions. The as-received fibers had the usual nodular or corn cob appearance. After removal of 13 μm (0.5 mils) off the diameter by electropolishing, examination of the surface showed it to be smooth with little evidence of the nodules left. In contrast, the nitric acid-etched surfaces, after removal of a similar amount, were considerably rougher with the nodules clearly evident.

Specimen Description

The specimens tested were 102, 142, and 203 μm (4, 5.6, and 8 mil) boron on tungsten fibers made by Avco Systems Division. The 102 and 142 μm fibers were made in a single-pass BCl_3-H_2 reactor using resistive heating of the fiber. The 203 μm fibers were also made in a single pass BCl_3-H_2 reactor with addition of VHF heating to supplement the resistive heating. A 12.7 μm (0.5 mil) diameter tungsten precursor was used to make the three fiber sizes. The maximum deposition temperature was near 1573°K (2372°F). The as-received tensile fracture strengths for these fibers were measured by Smith [4] and are shown in Table 1.

Table 1

Tensile Fracture Stresses of As-Received Boron Fibers [4]

Fiber Diameter		Average Fracture Stress		Coefficient of Variation
μm	(mils)	MN/m^2	(ksi)	%
102	(4.0)	3310	(480)	9.4
142	(5.6)	2880	(418)	13.5
203	(8.0)	3590	(521)	23.5

Analysis of the Data

From measurement of the change in length of the fiber with time of electropolishing of the fiber under test, the axial strain ε_z as a function of fiber radius r could be calculated. We assume that the mechanical properties of the boron do not depend on radius, that is, that both Young's modulus E and Poisson's ratio ν are constant, but we do allow the tungsten boride core to have properties different from the boron sheath. Witucki [1] has treated the case of equal moduli for both the core and sheath. We also assume that the axial strains are produced only by axial stresses. This means we have neglected the effects of σ_r and σ_θ stresses on the axial strain ε_z during the electropolishing process. The stress at a position in the as-received fiber of radius r_o is derived in the Appendix and is given by

$$\sigma(r_o, r) = -\left[(E_c - E_b)\frac{r_c^2}{r^2} + E_b\right] x \left[\frac{r}{2}\frac{d\varepsilon_z(r)}{dr} + \varepsilon_z(r)\right] \qquad (1)$$

where

E_c = Young's modulus of core

E_b = Young's modulus of boron sheath

r_c = radius of core

r = radius of electropolished fiber

$\varepsilon_z(r)$ = the axial strain at a fiber radius r with $\varepsilon_z(r_o) = 0$

DiCarlo [5] has shown that the core of the 203 μm (8 mil) fiber consists of two parts: a W_2B_5 inner core ~12.8 μm (0.5 mils) in diameter and a WB_4 outer core 17 μm (0.67 mils) in diameter. He reports average Young's moduli of the core borides and boron sheath to be 669 GN/m^2 (97 x 10^6 psi) for the W_2B_5, 407 GN/m^2 (59 x 10^6 psi) for the WB_4, and 393 GN/m^2 (57 x 10^6 psi) for the boron sheath. In Eq (1), we consider the outer core of WB_4 and the boron to have the same Young's moduli, thus

$$E_c = 669\ GN/m^2\ (97 \times 10^6\ psi)$$

$$E_b = 393\ GN/m^2\ (57 \times 10^6\ psi)$$

$$r_c = 6.4\ \mu m\ (0.25\ mils)$$

Experimental Results

Measurements were made on ten or more specimens of each of the three sizes of fibers. Fig. 2 is the plot of the raw data, that is, the strain along the fiber axis ε_z versus radius r for a 102 μm (4 mil) diameter fiber. This plot is typical of most of the runs except that most fibers broke before the core was reached. The fiber initially contracts as the surface is removed, then elongates, becoming longer than its original length. The test was terminated at a radius of 8.1 μm (0.32 mils) which is the approximate radius of the WB_4 the outer boride of the core. The electropolishing method used was not nearly as effective in removing the tungsten borides as it was in removing the boron sheath as indicated by a reduction in polishing current at the core diameter. From these data and Eq (1), the longitudinal stress $\sigma(r_o, r)$ at radius r for the as-received fiber at radius r_o could be calculated. Fig. 3 shows the results for the data of Fig. 2. The dashed portion of the curve indicates the average stress within the core. Details of how the stress varies with radius in the core region could not be obtained because the tungsten borides were ineffectively removed by the electropolishing

solution. Figs. 4 and 5 show the results for typical 142 μm (5.6 mil) and 203 μm (8 mil) boron fibers respectively. For both of these curves, the fibers broke before the core diameter was reached. For other runs for the 102, 142, and 203 μm (4.0, 5.6, and 8.0 mil) diameter fibers the shape of the curves were similar with variations of up to ±15% in the compressive stresses at the surfaces and the maximum tensile stresses near the core.

Discussion

The three sizes of boron fibers investigated show similar residual stress distributions; i.e., compressive at the surface, tensile near the core, and for the 102 μm (4 mil) fiber compressive again in the core. It is expected that the 142 μm (5.6 mil) and 203 μm (8 mil) fibers also would show compressive core stresses. Measurements made in Refs 6 and 7 of the curvature of split fibers 102 μm (4 mils) and smaller before and after removal of the tungsten boride core have shown the core to be in compression. Witucki [1] considers three sources of the residual stresses in the boron fibers: (1) the CVD process itself in which the boron is deposited with a biaxial deposition stress (such a stress might arise, for example, from surface tension or nodule growth effects), (2) the volume increase of the core due to the formulation of the tungsten borides, and (3) the difference in the thermal expansion between the boride core and the boron sheath. Other effects which contribute to the residual stresses are annealing of the disorder produced when the boron is deposited and creep and anelastic deformation [8] which would tend to relax the residual stresses. Considering only the deposition stress and assuming the core and sheath to be completely elastic with the same elastic constants, the axial stress is given by [1]

$$\sigma_z(r) = \sigma_d(1-2\ln\frac{r_o}{r}) \qquad (2)$$

where

$\sigma_z(r)$ = axial stress at radius r

σ_d = deposition stress

r_o = radius of boron fiber

r = radius at which stress is given

In Eq (2) if we let σ_d = -1300 MN/m^2 (-190 ksi), a surface stress typical of those measured in this investigation, $\sigma_z(r)$ increases much more rapidly with decreasing r than our measurements indicate. Such large stresses as predicted by Eq (2) will most certainly be relaxed due to creep in the boron sheath and possibly in the tungsten boride core at the temperature of CVD of the boron. We are, at present, investigating a model in which the stresses produced by the deposition process are allowed to relax by creep of boron sheath and boride core.

As the diameter of these fibers is reduced by etching or electropolishing, the fibers contract along their axis as a result of the removal of the compressive layers. This is shown in Fig. 2 for a 102 μm (4 mil) fiber. This contraction increases the compressive stress in the core. The tensile strength of fibers whose fracture is controlled by flaws in the core should thus show an equal increase in the core fracture stress upon etching. Smith [4] has measured the average tensile fracture strength of etched 203 μm (8 mil) boron derived from the same spool of material as was used in this investigation. He has shown that etching produces fibers which fracture in essentially all cases from core flaws. In Table 2 are shown the stresses calculated for the core at fracture using UTS data reported by Smith for various etched diameters. The Young's modulus for the core is the same as

that used in Eq (1). Also shown in Table 2 are the axial strains along with the resulting changes in the stresses at the core produced by electropolishing the 203 μm (8 mil) fiber whose stress distribution was shown in Fig. 4. We can compare the core fracture stress of Smith's work to the increase in core stress from this investigation by assuming the core fracture stress at zero strain to be 7.74 GN/m^2 (1122 ksi). This core fracture stress for as-received fibers is larger than the value 7.21 GN/m^2 (1045 ksi) derived from Smith's work. The lower value found by Smith can be attributed to surface flaws and to effects caused by the rough nodular surface at the as-received fibers. Fig. 6 is a plot of the diameter dependence of the core fracture stress as derived from Ref 4 and from the axial strain measured in this investigation. The close agreement between Smith's fracture stress data and the data of this investigation supports Smith's argument that the increase in UTS is due to the increase in the compressive stress at the core produced by the fiber contraction during surface removal.

Table 2

Core Fracture Stresses of Etched and Electropolished 203 μm (8 mil) Boron Fibers

Etched Dia. (2r) μm	(mils)	Fiber Stress at Fracture [4] (σ_f) GN/m^2	(ksi)	Core Stress[1] at Fracture (σ_c) GM/m^2	(ksi)	Axial Strain[2] (ε_z) mm/m	Change in Core Stress[3] ($\Delta\sigma_c$) GN/m^2	(ksi)	Calc. Core Fracture Stress[4] ($\sigma_{c\ calc.}$) GN/m^2	(ksi)^z
203	(8.00)	4.25	(616)	7.21	(1045)	0	0	(0)	7.74	(1122)
188	(7.42)	4.71	(683)	7.99	(1159)	-0.373	-0.25	(-36)	7.98	(1158)
174	(6.86)	4.79	(694)	8.12	(1177)	-0.690	-0.46	(-67)	8.20	(1189)
164	(6.45)	4.92	(714)	8.34	(1210)	-0.887	-0.59	(-86)	8.33	(1208)
138	(5.45)	5.03	(730)	8.52	(1235)	-1.260	-0.84	(-122)	8.58	(1244)
114	(4.50)	5.23	(759)	8.83	(1281)	-1.512	-1.01	(-147)	8.75	(1269)
90	(3.55)	5.30	(768)	8.89	(1290)	-1.685	-1.12	(-163)	8.86	(1285)

(1) $\sigma_c = E_c \sigma_f / [E_c r_c^2/r^2 + E_b (1 - r_c^2/r^2)]$

(2) The strains are those measured in this investigation for the 203 μm (8 mil) fiber after electropolishing.

(3) $\Delta\sigma_c = \varepsilon_z E_c$

(4) $\sigma_c^{calc.} = 7.74 + |\Delta\sigma_c|$ GM/m^2

An expression is derived which is used to calculate the longitudinal residual stress $\sigma(r_o, r)$ at radius r for an as-received fiber of radius r_o from measurements of the axial strain produced by removal of the surface by electropolishing. In deriving this expression, we neglect the effects due to radial and tangential stresses. The original fiber is considered to consist of a core of radius r_c and sheath with Young's moduli E_c and E_b, respectively. Consider the fiber to be electropolished to a radius of r, then the stress in the surface layer will be $\sigma_s(r)$. If a layer of thickness Δr is removed by electropolishing, a force ΔF is removed from the remaining fiber or

$$\Delta F = - \sigma_s(r) 2\pi r \Delta r \tag{A1}$$

This force produces an axial strain of $\Delta\varepsilon$, or

$$\Delta\varepsilon = \frac{\Delta F}{E_c \pi r_c^2 + E_b \pi (r^2 - r_c^2)} \tag{A2}$$

Combining Eqs (A1) and (A2) and solving for $\sigma_s(r)$ we have

$$\sigma_s(r) = - \frac{\Delta\varepsilon}{\Delta r} \times \frac{E_c r_c^2 + E_b (r^2 - r_c^2)}{2r} \tag{A3}$$

When $r = r_o$, we let $\varepsilon = o$. The stress $\sigma_s(r)$ is the stress derived from the stress distribution $\sigma(r_o, r)$ of the as-received fiber plus the stress produced in the remaining fiber by the strain ε or

$$\sigma_s(r) = \sigma(r_o, r) + \varepsilon \left[\frac{E_c r_c^2 + E_b (r^2 - r_c^2)}{r^2} \right] \tag{A4}$$

Combining Eqs (A4) and (A3), we have

$$\sigma(r_o, r) = - \left[(E_c - E_b) \frac{r_c^2}{r^2} + E_b \right] \times \left[\frac{r}{2} \frac{d\varepsilon}{dr} + \varepsilon \right]. \tag{A5}$$

REFERENCES

[1] Witucki, R. M., "High Modulus, High Strength Filaments and Composites," Technical Report AFML-TR-66-187. Air Force Materials Laboratory, Dayton, Ohio, 1967.

[2] Faughnan, K. A., Proceedings of the Twenty-Ninth Annual Conference of the Wide World of Reinforced Plastics, Society of the Plastics Industry, Inc., New York, 1974, pp. 4-B,1 to 4-B,10.

[3] Diefendorf, R. J., "Research on Improved High Modulus, High Strength Filaments and Composites Thereof," Technical Report AFML-TR-65-319, Air Force Materials Laboratory, Dayton, Ohio, 1965.

[4] Smith, R. J.: "Changes in Boron Fiber Strength Due to Surface Removal by Chemical Etching," to be published, NASA TN.

[5] DiCarlo, J. A.: Private communication.

[6] Talley, C. P., "High-Modulus, High-Strength Reinforcements for Structural Composites," Technical Report ML-TDR-64-88, Part III, Air Force Materials Laboratory, Dayton, Ohio, 1965.

[7] Berry J. M., "Research on Improved High Modulus, High Strength Filaments and Composites Thereof," Technical Report AFML-TR-66-98, Air Force Materials Laboratory, Dayton, Ohio, 1966.

[8] DiCarlo, J. A., "Composite Materials: Testing and Design," (Fourth Conference), American Society for Testing and Materials, Philadelphia, 1976.

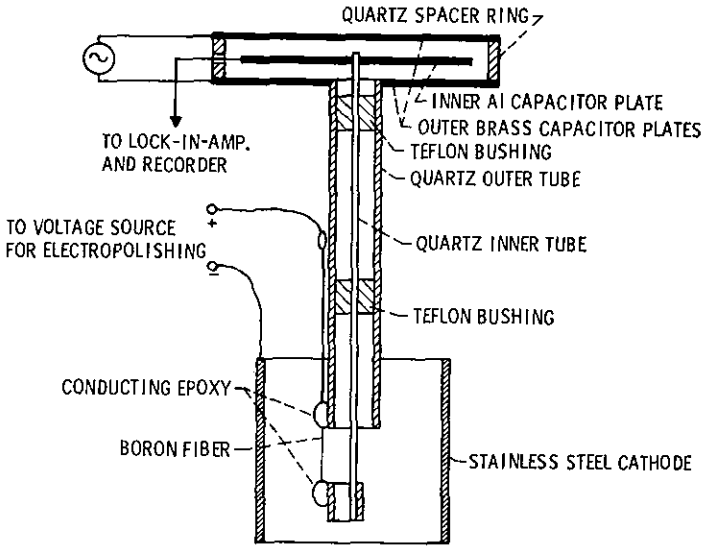

Figure 1. - Quartz gauge used to measure length change of a boron fiber specimen.

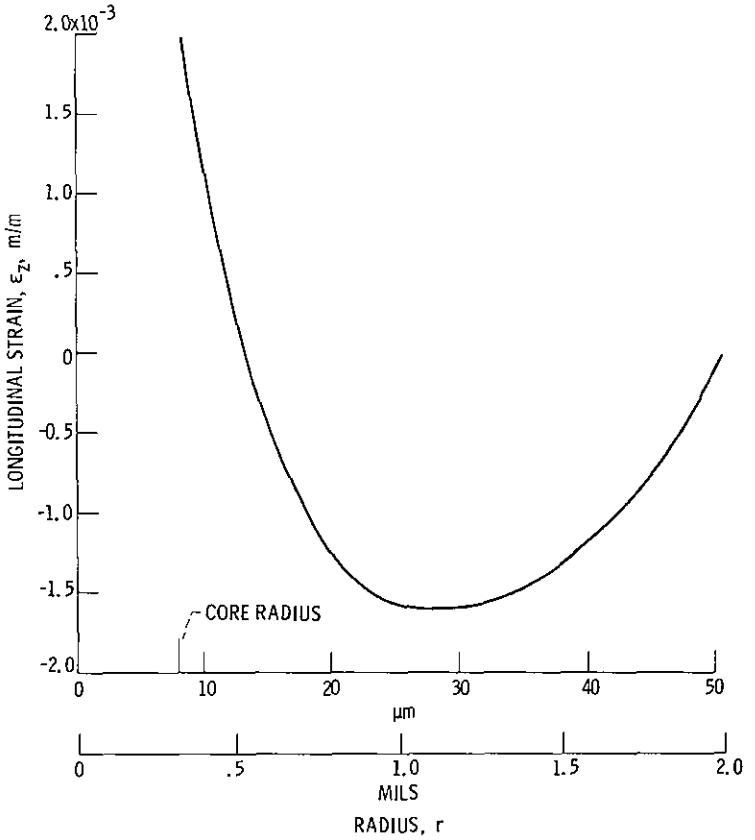

Figure 2. - Longitudinal strain versus electropolished radius of 102 μm (4 mil) diameter B/W fiber.

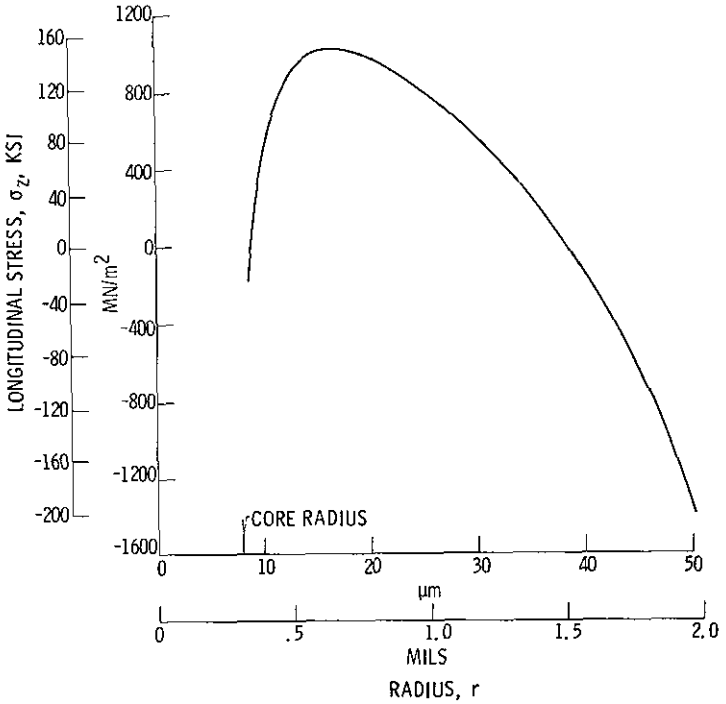

Figure 3. - Longitudinal residual stress distribution in 102 μm (4 mil) diameter B/W fiber.

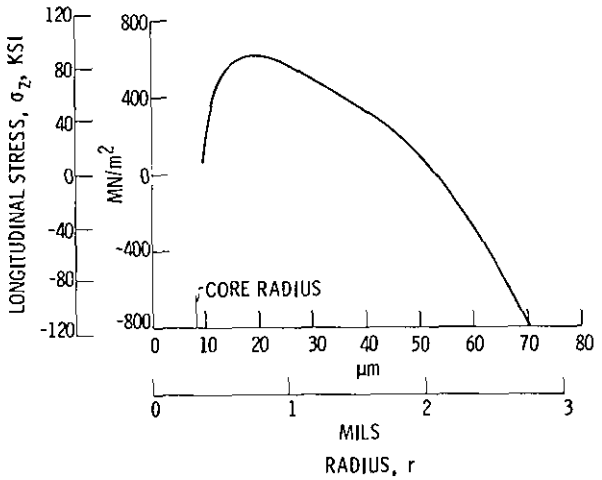

Figure 4. - Longitudinal residual stress distribution in 142 μm (5.6 mil) diameter B/W fiber.

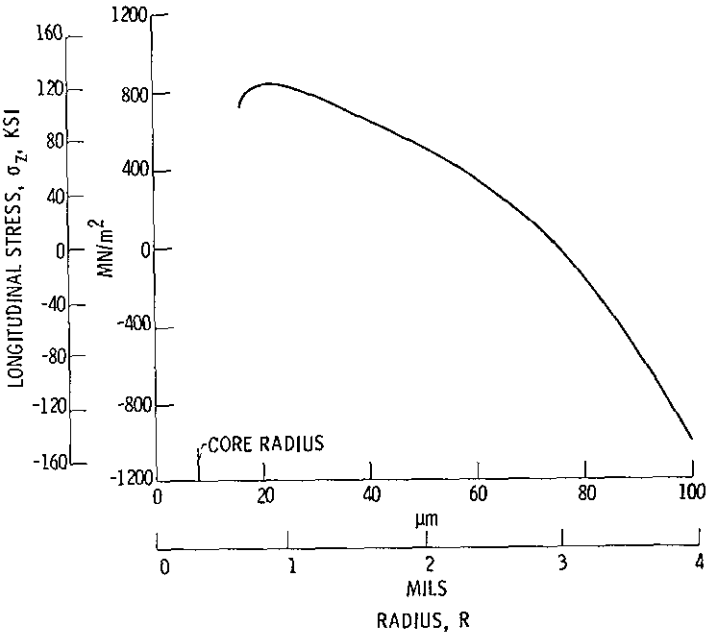

Figure 5. - Longitudinal residual stress distribution in 203 μm (8 mil) diameter B/W fiber.

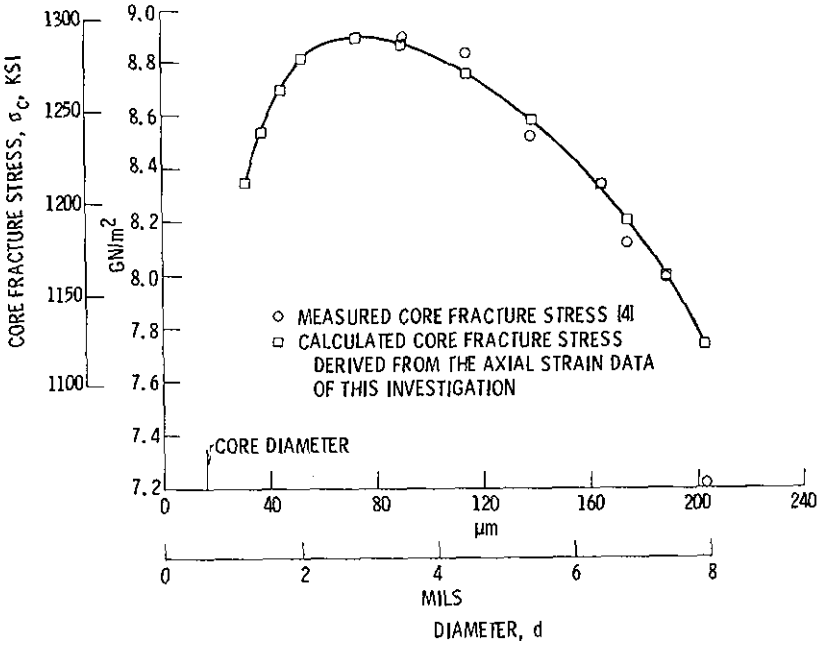

Figure 6. - Diameter dependence of the core fracture stress of 203 μm (8 mil) B/W fiber derived from Smith's UTS data [4] and from the axial strain measurement of this investigation.

NASA-Lewis